

NO. 179 OBSERVATIONS OF THE SOUTH EQUATORIAL BELT
DISTURBANCE ON JUPITER IN 1971

by Stephen M. Larson

March 1972

ABSTRACT

Some aspects of the major South Equatorial Belt disturbance of 1971 are described from photographic observations obtained at the Catalina and Bosscha Observatories. The motions of several spots produced by the disturbance during the first two months of activity were measured. The projection comparator used for measurement is also described.

1. Introduction

Starting in late June 1971 the appearance of Jupiter was remarkable for the great amount of activity associated with the recurrence of a major disturbance in the South Equatorial Belt (SEB). These major disturbances are marked

by violent meteorological activity that changes the appearance of a large area in a relatively short time. The extent of activity in each disturbance was varied. The most active one occurred in 1928, followed by one in 1943 (Reese and Chapman 1968), and the present one. The sequential development of a "typical" SEB disturbance has been documented (Peek 1958, Reese and Chapman 1968), and the 1971 disturbance was fairly typical. Because the SEB disturbance affected some 20° of latitude in the Southern Hemisphere, the SEB region has been divided into three sections or "branches": the SEBs (-19°), the SEBZ (-14°), and the SEBn (-8° Zenographic latitude) (Reese 1972). The spread of activity in longitude of the disturbance was due in part to differential rotation of these branches.

2. The Observations

The routine program of planetary photography was in progress at the 154-cm reflector of the Catalina Observatory on June 21, 1971 when Visiting Astronomer W. E. Fox, Director, Jupiter Section, B. A. A., noted a *small white spot in the bright SEBZ*. The other observers were alerted to the possibility of the importance of this object, and the photographs obtained by R. B. Minton on that night recorded the spot (Minton 1972). The outbreak was later announced by Reese in IAU Circular 2338 and the small spot was found on photographs in the ultraviolet reported by Baum (1971) as part of the NASA Planetary Patrol on June 18, 1971.

Thereafter, with increased emphasis on Jupiter photography, high-resolution coverage was obtained of the early development until the rainy season severely limited coverage in mid-July. At about this time, J. W. Fountain was starting an observing run at the Bosscha Observatory in Lembang (Java), Indonesia, (Larson 1971) for direct photography of Mars during the very favorable opposition. While in Java, he obtained over 3,000 images of Jupiter in several wavelength bands with the twin 60-cm refractor.

Together, the data obtained at the Catalina and Bosscha Observatories provide enough coverage to study the motions of several features produced by the disturbance. Figures 1-4 show 22 photographs of the planet (all composites) selected from both observatory collections, to illustrate the Disturbance during the period July 14-October 4, 1971. Reference is made to R. B. Minton's *LPL Comm. No. 178* for illustrations during the first 19 days following the eruption (these were all obtained at the Catalina Observatory). Table I lists the times and emulsion data for the 22 photos in Figures 1-4.

Measurements on individual features of the disturbance are shown graphically in Figure 5, expressed in System II. They cover the period June 21-August 20, 1971. The measurements were made with the comparator shown in Figures 7 and 8, below.

The relative velocities of the features in a particular latitude region have been shown to vary with time (Chapman 1969), making the determination of rotation as a function of latitude difficult. In addition, the developmental changes in the shape of a feature can introduce irregularities in the apparent motion. Still, events producing features whose identities are certain for several weeks, such as the SEB disturbances, presently offer the best opportunity for studying currents in the Jovian atmosphere. Figure 6 shows the average rotation period of several observed features belonging to the 3 latitude regions of the disturbance.

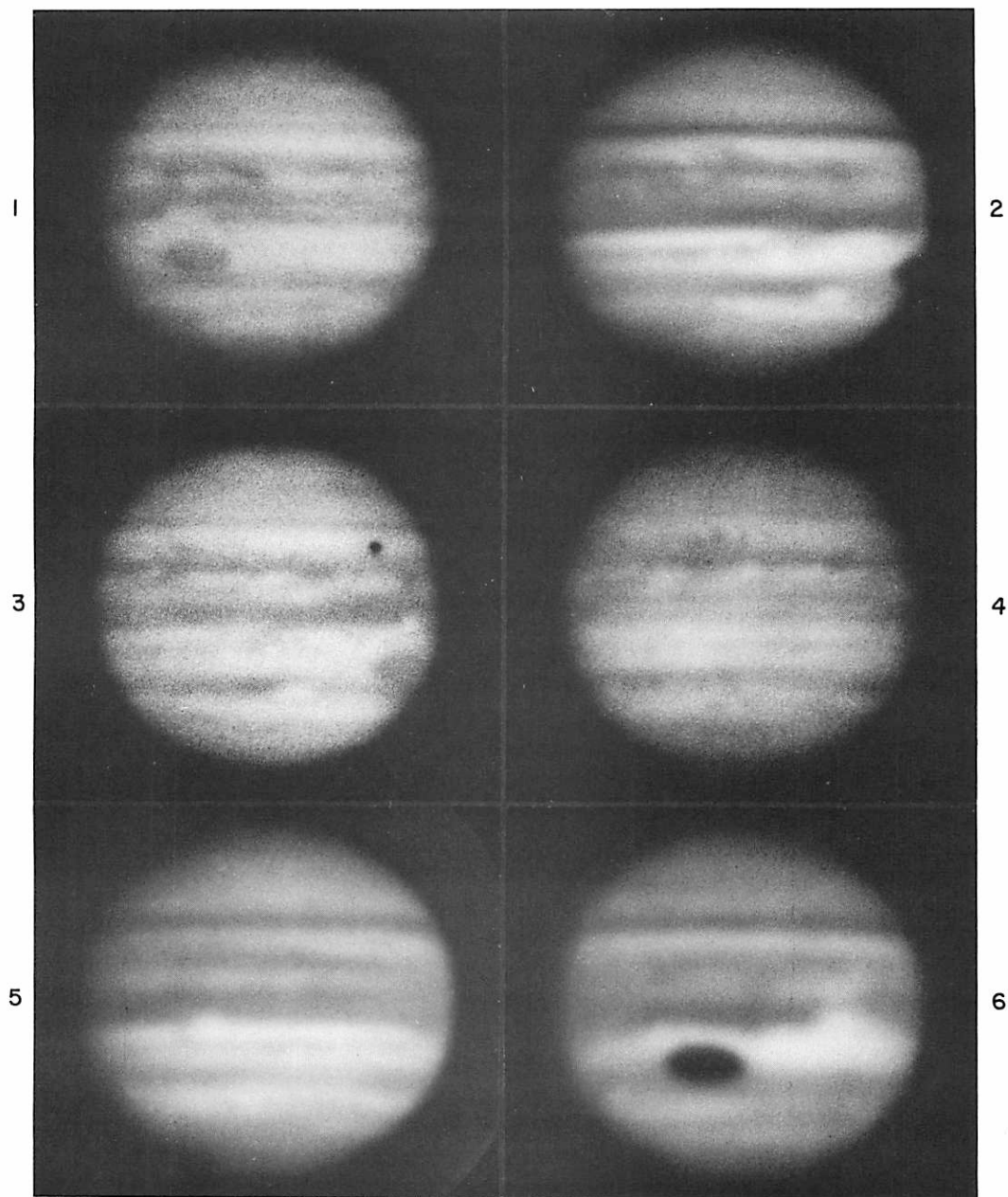


Fig. 1 Image No. 1: July 14, red. Large bay N of RS (Feature A in Fig. 5).
 No. 2: July 15, blue. Dark spots in SEBs not as distinct. SEBs appearing
 more continuous than in No. 3. No. 3: July 15, red. Spot A (Fig. 5) is N
 of RS. Dark spots in SEBs. No. 4: July 18, red. Outbreak of second dis-
 turbance seen as small white spot in SEBZ after being overtaken by leading
 edge of SEBs spot. No. 5: July 20, blue. Column joining SEBs and SEBn
 shown adjacent to second disturbance. No. 6: July 24, blue. Activity
 spreads in SEBn as leading white spot A moving away from RS.

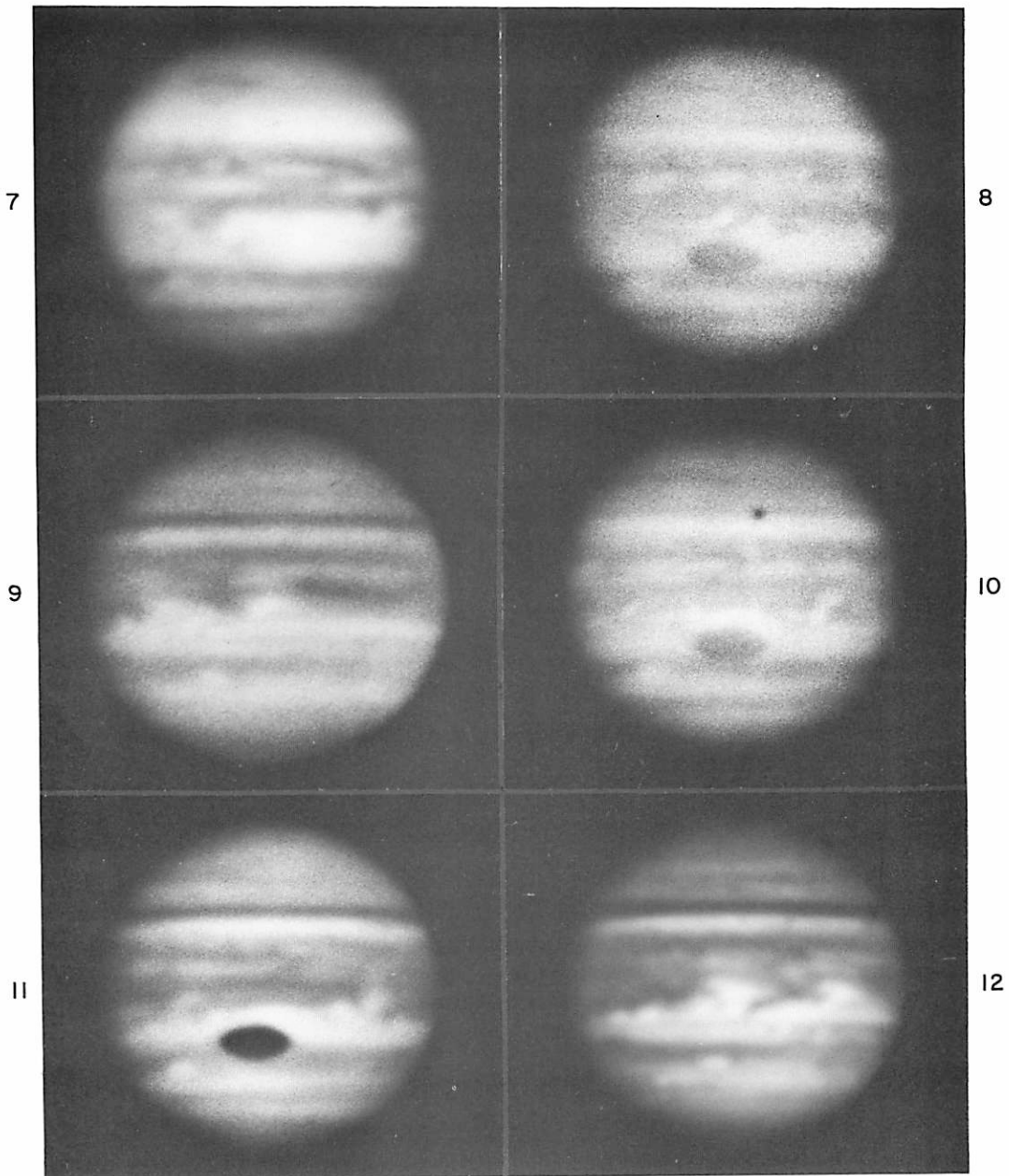


Fig. 2 Image No. 7: July 24, near-IR. RS is nearly invisible in near-IR; compare with No. 6. No. 8: July 29, red. Spectacular wisps from N of RS in SEBs. No. 9: Aug 2, blue. Large white spots A and C (Fig. 5) disrupt appearance of SEBn. No. 10: Aug 3, red. Object B of Fig. 5 extends deep in SEBn. No. 11: Aug 5, blue. Compare with No. 10, similar longitude. No. 12: Aug 7, blue. Comparison between this image (and 12 α) and No. 13 (plus 13 α) indicates large differences.

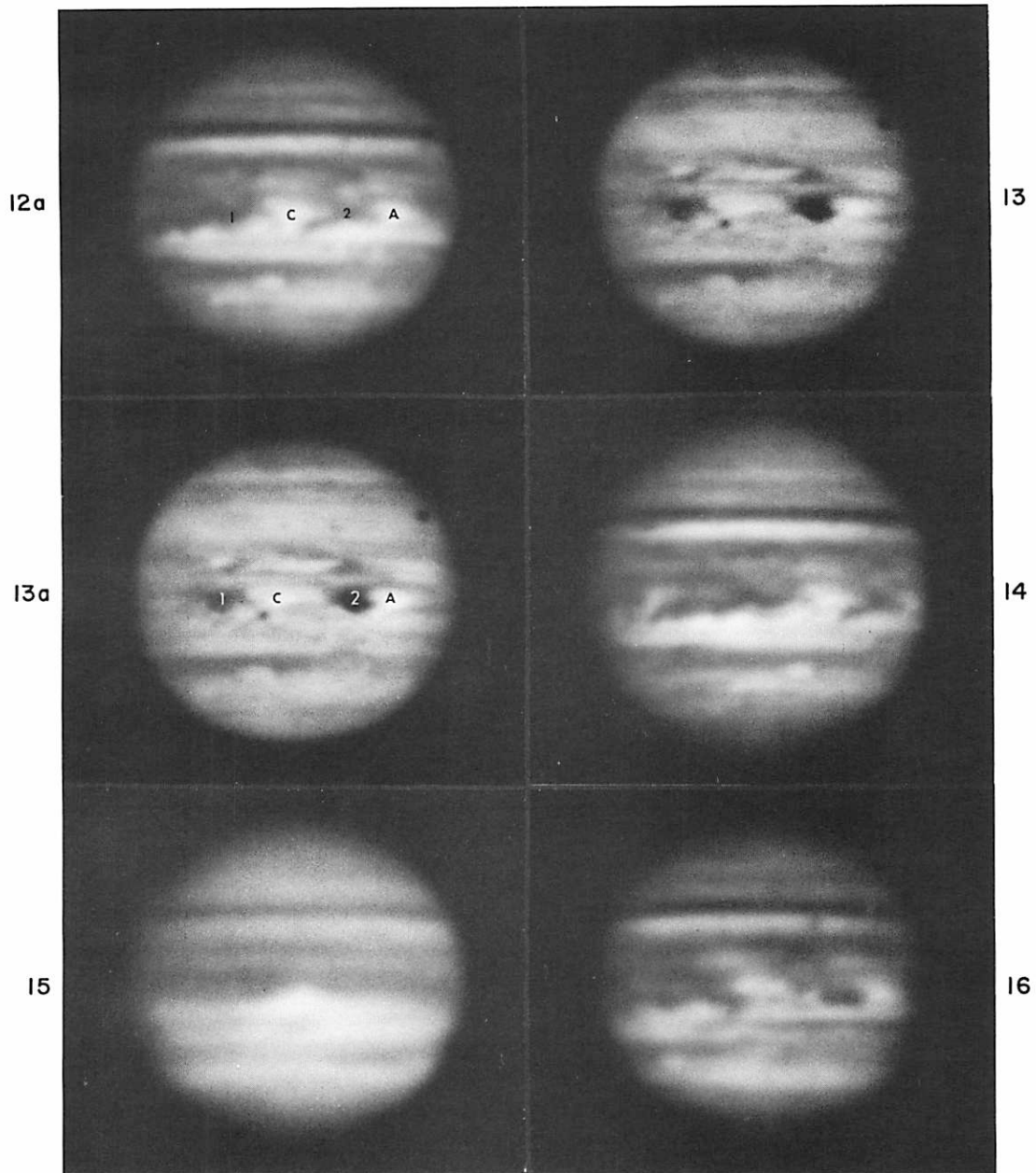


Fig. 3 Image No. 12a: Aug 7, blue (same as No. 12). Features labelled A and C, shown in Fig. 5, are identified. (Features 1 and 2 not shown in Fig. 5 but used in comparison with No. 13a). No. 13: Aug 7, near-IR. Repeated with identifications in 13a. Blue features 1 and 2 very dark in near-IR; their blue color is shown on simultaneous color records. No. 14: Aug 7, blue. Spots A and C of No. 12a have moved 1 cm to right; similar spot, called B in Fig. 5, has appeared 1 cm from left limb. No. 15: Aug 8, blue. Spot D (of Fig. 5) prominent on CM in SEBn. No. 16: Aug 14, blue. Longitude similar to No. 12a, with Spots A and C shown (modified).

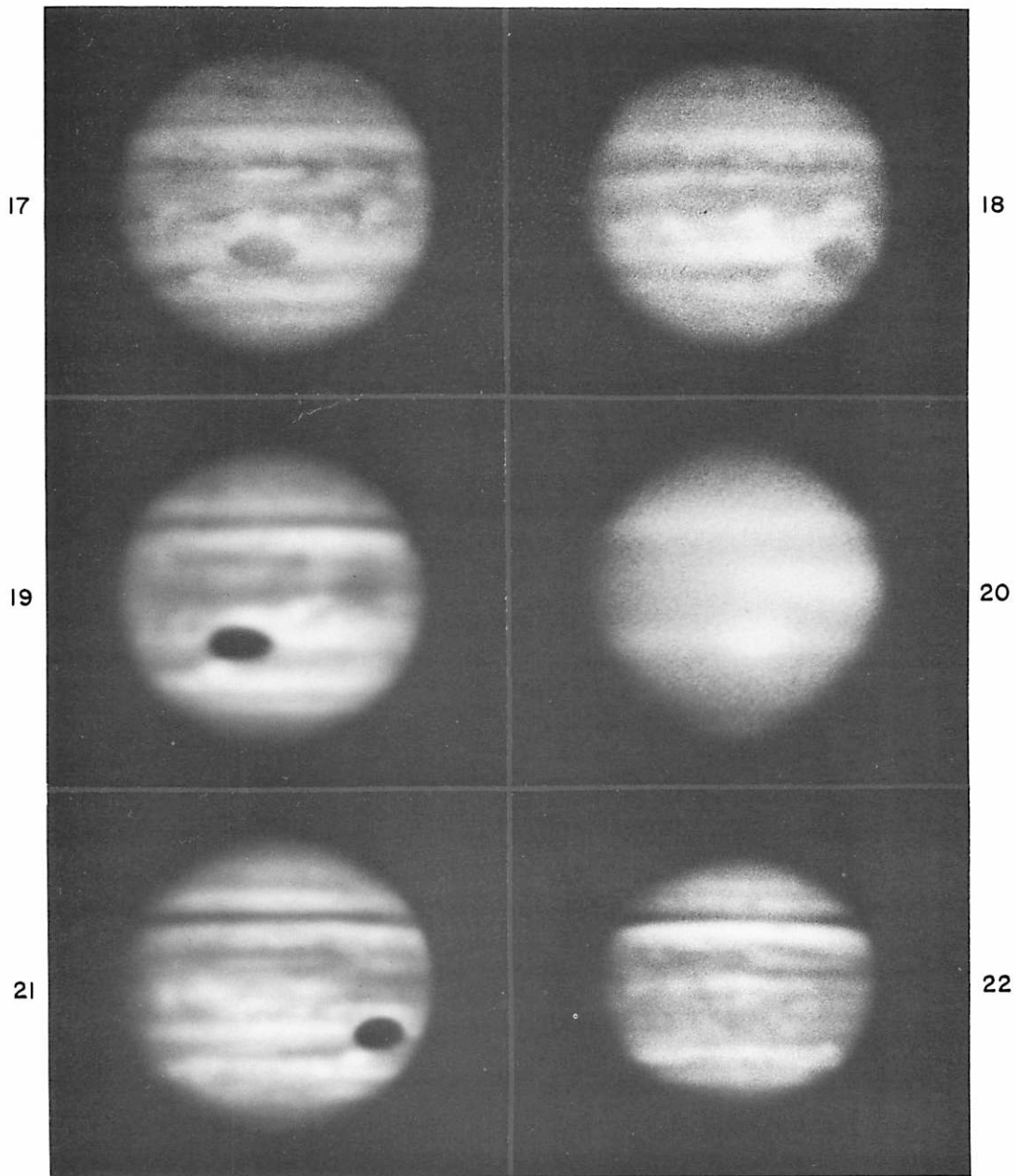


Fig. 4 Image 17: Aug 15, red. Taken 12 days after No. 10, with equatorial detail enhanced. No. 18: Aug 20, red. Note bright bay in SEBn. No. 19: Sept 3, blue. RS still prominent, contrary to case histories of other major eruptions. No. 20: Sept 3, methane filter. RS appearance normal but EW gradient across equatorial region. No. 21: Sept 6, blue. RS still prominent despite train of small dark spots in SEBs having by then drifted past RS. No. 22: Oct 4, blue. Disturbance in equatorial region diminished. NTrZ unusually bright.

TABLE I

Observational Data on Photographs

Fig.	Date 1971	Time (UT)	Film	Filter	CM II	Obsy.*	Compos. No.	No. Images
1	July 14	15:40.7	4-X	OG-5	347.1	Bo	1370	4
2	July 15	14: 8.5	103-0	BG-3	81.2	Bo	1374	3
3	July 15	13:33.2	4-X	OG-5	60.0	Bo	1373	6
4	July 18	12:54.8	4-X	OG-5	127.6	Bo	1379	6
5	July 20	14:22.9	103-0	BG-3	121.3	Bo	1381	6
6	July 24	4:20.5	103-0		357.9	Ca	1501	5
7	July 24	4:46.2	HSIR	GG-14	13.4	Ca	1502	5
8	July 29	13:40.7	4-X	OG-5	8.5	Bo	1389	4
9	Aug 2	3:46.5	103a-0		249.0	Ca	1545	2
10	Aug 3	12:51.7	4-X	OG-5	8.9	Bo	1391	4
11	Aug 5	4:27.9	103a-0		4.6	Ca	1503	3
12	Aug 7	3: 9.7	III-0		257.6	Ca	1505	6
12a	Aug 7	3: 9.7	III-0		257.6	Ca	1505	6
13	Aug 7	3: 3.3	HSIR	RG-5	253.6	Ca	1504	5
13a	Aug 7	3: 3.3	HSIR	RG-5	253.6	Ca	1504	5
14	Aug 7	3:48.7	III-0		280.9	Ca	1506	4
15	Aug 8	14:15.5	103-0	BG-3	90.5	Bo	1393	4
16	Aug 14	3: 4.6	III-0		225.6	Ca	1507	4
17	Aug 15	12:38.9	4-X	OG-5	2.8	Bo	1403	6
18	Aug 20	13: 6.7	4-X	OG-5	50.3	Bo	1420	3
19	Sept 3	3:21.2	III-0		357.2	Ca	1511	5
20	Sept 3	3:56.9	HSIR	CH ₄	19.2	Ca	1510	5
21	Sept 6	2:19.9	III-0		50.9	Ca	1512	4
22	Oct 4	1:45.5	103-0		271.6	Ca	1514	6

*

Ca = Catalina; Bo - Bosscha

3. Description of the Disturbance

Before the outbreak, the Red Spot (RS) was very prominent and the SEB Zone (SEBZ) was very bright and free of detail. The SEBs was very weak, appearing only as a poorly defined grey line in the best photographs. Because of the faintness of the SEBs, the SEBZ and the South Tropical Zone (STrZ) combined to form the brightest region on the planet. As stated, the actual outbreak started as a small white spot that later developed a darker border and a small grey column on a side of increasing longitude, connecting the SEBn with the SEBs. White spots later appeared near the position of the first spot and accumulated until being caught in the current of the SEBn. The point where the dark column connected with the SEBs emitted dark spots that travelled along the SEBs in the direction of increas-

ing longitude. These so-called retrograding* dark spots spread out in longitude so that in a few weeks the whole S equatorial region was a confusing mass of spots and other detail. Just less than a month after the first outbreak, the second disturbance appeared as another spot and column at a longitude just overtaken by the SEBs dark spots. A second disturbance source was also observed during the 1943 disturbance. By the middle of August, virtually the whole planet between the equator and -20° was affected, producing a very unsettled appearance.

4. The SEBZ

The outbreak appeared in the SEBZ near -14° (Zenogr.) and 79° System II longitude. The activity in the SEBZ was confined to the formation of white spots that generally drifted towards the SEBn, and dark columns bridging the SEBs and SEBn. The first white spot (A in Fig. 5) appeared and drifted slowly in longitude ($0.9^\circ/\text{day}$) and latitude, until about July 6. The influence of the SEBn current took hold and the spot accelerated, attaining a new drift rate of $5.3^\circ/\text{day}$ with respect to System II. Later, apparent changes in this period seemed to result in a small latitude change, partly due to the fact that as the spot grew its boundary became less distinct. The average period of these white spots was $9^{\text{h}}52^{\text{m}}27^{\text{s}}$.

One notable spot (C in Fig. 5) formed very rapidly between July 24 and 26 in front of spot A, illustrating the extent of the unstable meteorological conditions brought about by the disturbance.

The dark columns appeared grey at first, but as they developed took on the yellow-brown color of the SEBn, as though material in the SEBn was being transported across the SEBZ into the SEBs where it may have developed into the SEBs spots. The change in the shape of the first column was due in part to the shear produced by the change in rotation period over the latitude it spanned. The curved shape of the column on July 7 represents the drift since June 23, when nearly the whole column was at the same longitude. The second disturbance had also formed a column (cf. Figs. 4, 7, 10, and 12 of *LPL Comm. No. 178*) by July 20, only two days after the outbreak. At times other column-like features crossed the SEBZ, but they were not associated with any disturbance-related spots.

After the disturbance was well developed, several dark spots and wisps, generally poorly defined and difficult to follow, appeared in the SEBZ.

5. The SEBn

The SEBn became a complicated mass of detail as a result of the white spots. The most dramatic aspect, however, may have been the distribution of colors. Strong blue and orange colors existed in unusual profusion. The uneven distribution is also evident in the 8900\AA methane band (Fig. 4, No. 20) where the absorption varies from E to W to a much greater extent than from the usual expected phase exaggeration produced by limb darkening.

* Although they are "retrograding" with respect to the arbitrary System II period, they of course rotate in the same direction as all other features on the planet. A "Westward drift" would be more descriptive.

As the disturbance progressed, spots in the SEBn protruded Northwards to the equator, and it became evident that much of the energy released in the Jovian atmosphere by the disturbance was directed to this region. As the activity of the disturbance died down, the scale of the detail diminished and became more uniform over the whole SEB.

6. The SEBs

When the column in the SEBZ reached the latitude of the SEBs, the current (slow with respect to System II) appeared to tear off pieces of the column producing dark spots. Most of the time the SEBs appeared more continuous in blue light than in red where the individual spots were well-defined. The spots varied in size but because of the lack of consistent resolution, it is impossible to tell if there was a size-lifetime correlation. The larger spots protruded to the S of the SEBs, their Northern edges always being close to -19° Zenographic latitude. The average period of SEBs spots was $9^{\text{h}}58^{\text{m}}24^{\text{s}}$, but those appearing before July 20 had average periods of $9^{\text{h}}58^{\text{m}}45^{\text{s}}$, while those appearing after July 20, $9^{\text{h}}57^{\text{m}}47^{\text{s}}$.

It was probably coincidental that the leading spots at the time had just passed the longitude of the second disturbance when it broke out. Spots produced by the second disturbance could not be identified as such because of the presence of spots produced by the primary disturbance. Reese (1971) predicted that by late August, the spots would reach the longitude of the RS and that as in the earlier major disturbances, the RS would fade. Although it could be seen that the spots were deflected Northwards by the RS hollow, the visibility of the RS did not diminish, and at this writing is still quite prominent.

7. Discussion

The appearance of the SEB disturbances seems to indicate a nearly cyclic release of energy built up in the lower levels of the Jovian atmosphere. With the internal heat providing the source from which the internally driven meteorology can take place (Kuiper 1972), it is likely that there exists unstable regional energy stores built up under a temperature inversion in the H_2O region that are released periodically. Reese (1972) has shown a correlation between (a) the longitudes of the three possible sources rotating close to the dekametric radio period and (b) the level of activity of the disturbances. The systematic location of the disturbance sources lends strong evidence that "sources" act as triggers for the release of energy to the upper atmosphere. The images taken in the 8900\AA methane band (Minton 1972) show the region of the outbreak as being either high, or at least free, of the methane gas that generally exists at the higher atmospheric levels. This can be caused by high local vertical velocities, and the varied distribution of colored material in the disturbed region probably represents vertical mixing and possible chemical reactions of different ammonium polysulfides normally present at various layers in the upper atmosphere.

8. The Projection Comparator

A simple instrument was constructed that allows easy measurements of planetary features by projecting a photograph of the planet coincident with an image of a coordinate grid of the appropriate parameters plotted by computer (Fig. 7). Basically, it is a comparator combining two optical systems with control for orientation, position, scale, and intensity differences. The main design constraint was that it accommodate the five-image strips of 35-mm film resulting from the planetary photography program, and that it be as compact and easy to construct as possible.

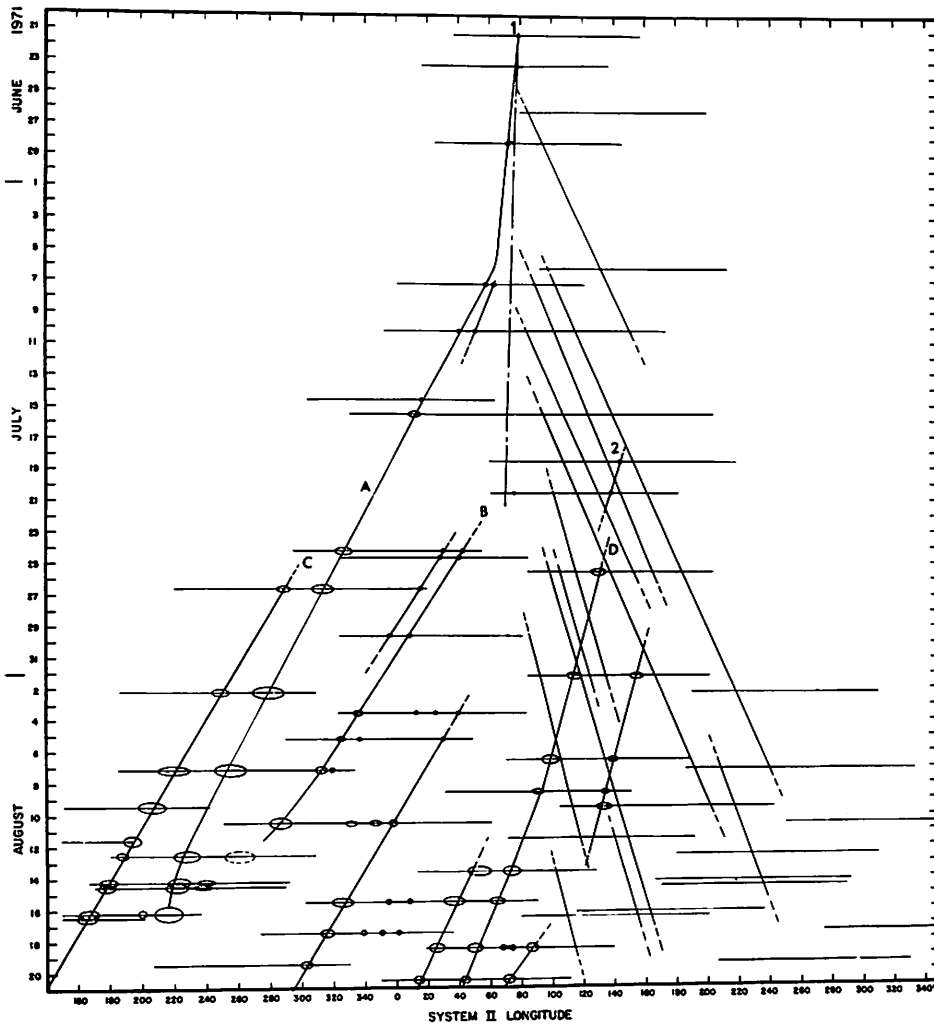


Fig. 5 Drift of features produced by SEB disturbance in System II ($9^{\text{h}}55^{\text{m}}42^{\text{s}}$). Positive slopes indicate motions in SEBn branch, usually by white spots. Dark spots in SEBs have longer periods, thus negative slopes. Beginning of primary disturbance indicated by 1, of second by 2. Nearly-vertical line would represent System III period ($9^{\text{h}}55^{\text{m}}30^{\text{s}}$), close to that of primary source. Small ellipses are observed dimensions of white spot (in x, y). Horizontal lines show longitude intervals observed.

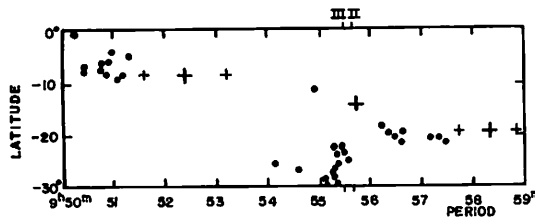


Fig. 6 Rotation period vs. Zenographic latitude determined from 1917-66 and 1971. Heavy crosses are average values and smaller crosses, extreme values, for 1971 disturbance. Dots are values given greatest weight from 1917 to 1966 by Chapman (1969). System II and III periods are marked in margin.

Figure 7 shows the viewing screen that displays the combined images enlarged to about 60 mm. The controls for image and grid brightness can be seen, as well as the film holder and y-coordinate adjustment screw on the side. X-coordinate adjustments are made by sliding the film holder in its guides.

The optical components can be seen in Figure 8. The projector lens for the planet has a variable focal length (4 to 6 inches) to produce an image the same scale as the grid. The scale variation over the field introduced by the optical aberrations were found to be negligible within the 2-inch radius used. A well-corrected enlarger lens projects the grid.

The grids are photographed from a computer-plotted grid on high-contrast litho film on a dimensionally-stable base to a standard size, and either aligned in the holder such that a right ascension reference trail can be lined up with reference lines on either side of the grid, or rotated on the grid holder a pre-computed amount by means of a circle graduated in degrees. The grids are computed in either centric, graphic, or eccentric form by an IBM 1130 computer with a 1627 plotter, with latitude and longitude circles drawn every 10° .

The image is aligned with the grid by movement in the appropriate x-, y- directions and enlarged to fit the grid either by eye or by means of some scale reference such as a double star. In the most common case of the planet showing a phase, the limb not affected by a terminator is used for alignment with the grid to minimize phase error. The greatest source of error is in aligning images of Jupiter when the limb-darkening prevents a well-defined limb, or in less than optimum exposure of images such that photographic effects minimize or exaggerate the limb.

In practice, it was found that measures of well-defined features on Jupiter were repeated to within $\pm 1^\circ$ in longitude within 30° of the center, and $\pm 2^\circ$ out to 60° , although these values vary considerably depending upon their visibility (contrast) and extent of the object. Consequently, with their different limb darkening, images taken in the short wavelengths are easier to position and give better results, than images taken in long wavelengths.

The ability to vary the intensity of the images independently optimizes the visibility of the features. Since the grid is light with no background, it does not cover up features. Even if the feature has very low contrast, the operator can turn off the grid, set a pointer such as a pencil on the screen at the position of the feature, and then turn on the grid to read the position. Although this arrangement works best for positive images, original negatives can also be used.

In addition, the comparator is well-suited for measuring Venus UV markings, clouds on Mars, and markings on Jupiter and Saturn where great accuracy is not required, and usually with a minimum of computer time devoted to such programs.

Acknowledgments: I wish to thank J. W. Fountain and R. B. Minton for use of the data they obtained at the Bosscha and Catalina Observatories, respectively. J. Barrett made the composites of Jupiter used in this paper. The Planetary Photography Program is supported by NASA Grant No. NGL-03-002-002.

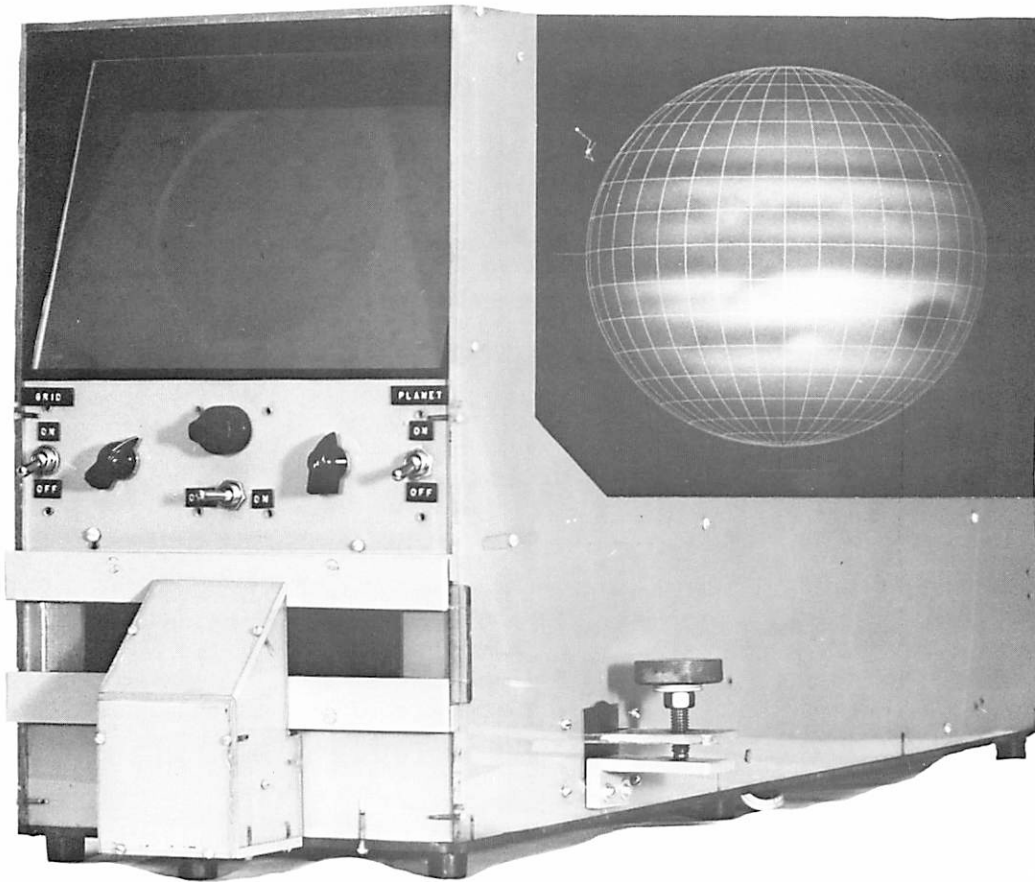


Fig. 7 The projection comparator controls and viewing screen, with the image of Jupiter and grid as seen on the viewing screen

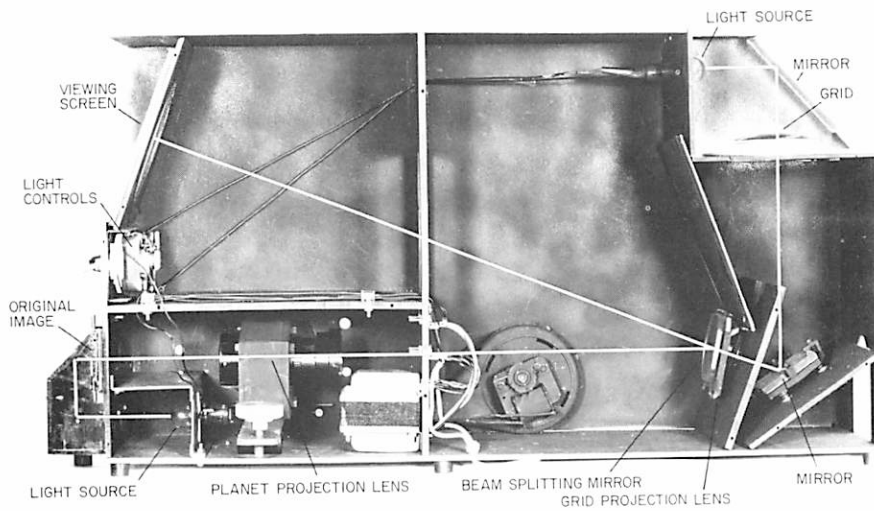


Fig. 8 The interior configuration of the projection comparator

REFERENCES

- Baum, W. A. and Reese, E. J. 1971, "Observations of New Major Disturbances on Jupiter", Observers Page, *Sky and Telescope*, 42, 176-180.
- Chapman, C. R. 1969, "Jupiter's Zonal Winds: Variation with Latitude", *Journal of Atmospheric Sciences*, 26, 198.
- Kuiper, G. P. 1972, "Planetary Studies at LPL: Jupiter", *Sky and Telescope*, 42, Jan and Feb, and *LPL Comm. No. 173*.
- Larson, S. M. 1971, "The Bosscha Observatory in Indonesia", *Sky and Telescope*, 42, 70-72.
- Minton, R. B. 1972, "Initial Development of the June 1971 SEB Disturbance on Jupiter", *LPL Comm. No. 178*.
- Peek, B. M. 1958, THE PLANET JUPITER, London (Faber and Faber).
- Reese, E. S. 1972, "Jupiter: Its Red Spot and Disturbance in 1970-71", *Icarus*, 17, 57-72.
- Reese, E. S., Chapman, C. R. 1968, "A Test of the Uniformly Rotating Source Hypothesis for the Southern Equatorial Belt Disturbance on Jupiter", *Icarus*, 9, 326-335.